Bocus, J., Agrafiotis, D., & Doufexi, A. (2018). Underwater Acoustic Video Transmission Using MIMO-FBMC. In *2018 OCEANS - MTS/IEEE Kobe Techno-Oceans (OTO)* Institute of Electrical and Electronics Engineers (IEEE). https://doi.org/10.1109/OCEANSKOBE.2018.8559160

Underwater Acoustic Video Transmission Using MIMO-FBMC

Mohammud J. Bocus, Dimitris Agrafiotis and Angela Doufexi
Department of Electrical and Electronic Engineering, University of Bristol, BS8 1UB, UK.

***Abstract*—In this paper we assess the transmission of a standard definition (SD) video over a 1000 m vertical time-varying underwater acoustic channel (UAC) using multiple-input multiple-output (MIMO) systems with spatial multiplexing gain. The MIMO systems are integrated with filter bank multi-carrier (FBMC) modulation and Orthogonal Frequency Division Multiplexing (OFDM) and their bit error rate (BER) performances are evaluated over the channel using preamble-based channel estimation. In this work we chose to use the FBMC system based on the Offset Quadrature Amplitude Modulation (OQAM) as it achieves maximum spectral efficiency. Simulation results show that MIMO-FBMC/OQAM provides a better error performance than MIMO-OFDM in the UAC, outlining its robustness against both time and frequency dispersions. Furthermore, the absence of a cyclic prefix (CP) in FBMC/OQAM implies that more useful bits can be transmitted per second, making it a better candidate than OFDM for transmitting real-time video with acceptable quality over a long acoustic link.**

I. Introduction

Over the past few years, a number of applications such as marine-life exploration and oil spillage monitoring have made underwater acoustic (UWA) communication an active area of research. Some applications require high quality real-time underwater wireless video transmission but this is very challenging due to the limited bandwidth in an underwater acoustic channel (UAC). In order to cope with the physical limitations of the UAC and simultaneously achieve a high data rate, technologies such as multiple-input multiple-output (MIMO) and orthogonal frequency division multiplexing (OFDM) have been investigated for UWA communication (e.g., [1]).

The channel impulse response (CIR) in an UAC is often very long, especially in shallow water where the direction of transmission is horizontal with respect to the sea floor. For an OFDM-based system, the cyclic prefix (CP) duration should be at least equal to the length of the CIR to avoid intersymbol interference (ISI). Consequently, in order to maintain a high bandwidth efficiency, the OFDM symbol duration should be made very long [2]. However, the variations across each OFDM symbol in a fast time-varying channel will result in performance degradation due to inter-carrier interference (ICI) caused by Doppler effect [2]. This drawback of OFDM has triggered research on another multi-carrier technique for UWA communication, namely filter bank multi-carrier (FBMC) modulation. The absence of a CP in FBMC implies that it offers a higher bandwidth efficiency than OFDM. Furthermore, in FBMC we can use filters which are well localized both in time and frequency to provide robust performance in doubly-dispersive UACs (e.g., [3]–[5]).

A particular communication scenario we are interested in consists of a remotely operated underwater vehicle (ROV) which communicates with a surface vessel over a long distance acoustic link. In order to maintain a vertical or near-vertical communication link (so as to minimize the effects of multipath propagation), an autonomous surface craft (ASC) which moves alongside the ROV can be deployed at the surface. The ASC can be equipped with the signal processing equipment such as acoustic modem and hydrophones. For this kind of application, it is expected that the uplink is used for transmitting multimedia data such as video while the downlink is used for sending control commands to the ROV (hence downlink requires much less bandwidth than the uplink). The data/video captured by the ASC can then be relayed to a ship or fixed platform such as an oil rig using radio waves.

MIMO-OFDM has been widely investigated for UWA communication and has been found to achieve good performance in terms of data rate and reliability (e.g., [1], [6]). FBMC systems based on Cosine modulated multitone (CMT) and Filtered Multitone (FMT) have only been recently considered for UWA communication (e.g., [3]–[5]). However, video transmission using spatially-multiplexed MIMO-FBMC systems is yet to be considered in an UAC. In this paper, we first evaluate the bit error rate (BER) performance comparison between MIMO-OFDM and MIMO-FBMC/OQAM in a vertical time-varying channel. Preamble-based channel estimation using the Interference Approximation Method (IAM) is considered for both systems. Video transmission is investigated with the MIMO-FBMC/OQAM systems since they not only provide the highest theoretical bit rates but also a better error performance. In terms of video compression technique, the H.264 Advanced Video Coding (AVC) standard is considered. Forward error correction (FEC) is used to reduce the number of bit errors which cause video packets to be dropped and consequently degrade video quality.

The paper is structured as follows: The characteristics of an UAC are described in Section II. The discrete-time baseband models for a single-input single-output (SISO) and MIMO FBMC/OQAM systems are provided in Section III. Section IV presents the performance evaluation of the systems in terms of bit error rate (BER), achievable bit rate and video transmission in a 1000 m vertical UAC. Finally conclusions are drawn at the end of this paper.

Notations:

Matrices and vectors are denoted by boldface uppercase and lowercase letters, respectively. The superscripts $(.)^T$ and $(.)^\star$

denote transpose and conjugate operations, respectively.

II. UAC Characteristics

The UAC is often described in literature as the worst channel in use today since it is severely affected by factors such as high transmission loss, ambient noise, multipath distortion, high propagation delays and Doppler spreading. The combined effect of these factors significantly limits the available bandwidth and also makes it dependent on both distance and frequency [7]. Hence the bandwidth for long range acoustic links (> 1 km) is usually in the order of a few kHz.

The transmission loss for a distance x and frequency f is computed as follows [8]

$$A(x,f) = x^k.\alpha(f)^x, \tag{1}$$

where $\alpha(f)$ is the absorption coefficient which can be computed in dB/km for f in kHz using the Thorp [9] or Fisher and Simmons [10] models and k denotes the geometrical spreading factor with values of 1 and 2 for shallow and deep water respectively.

Ambient noise, which is often referred to as colored noise, is mainly caused by turbulence (N_{tb}), breaking waves (N_w), shipping (N_s) and thermal (N_{th}) noise sources. These are defined by the following equations (f is in kHz) [8]

$$\begin{aligned} 10\log N_{tb}(f) &= 17-30\log(f) \\ 10\log N_s(f) &= 40+20(s-0.5)+26\log(f)-60\log(f+0.03) \\ 10\log N_w(f) &= 50+7.5w^{0.5}+20\log(f)-40\log(f+0.4) \\ 10\log N_{th}(f) &= -15+20\log(f), \end{aligned} \tag{2}$$

where s is the shipping factor with values between 0 and 1 for low and high activity respectively and w is the speed of wind in m/s. The overall power spectral density (PSD) of the ambient noise is expressed as follows [8]

$$N_{psd}(f) = N_{tb}(f)+N_s(f)+N_w(f)+N_{th}(f). \tag{3}$$

The speed of sound in water is about 200,000 times less than the speed of electromagnetic waves in air. Therefore the UAC experiences longer propagation delays than terrestrial radio links. A reasonable approximation of the speed of sound (v) in seawater as a function of the depth (z) in meters, temperature (θ) in degrees Celsius, and salinity (S) in parts per thousand is as follows [11]

$$\begin{aligned} v &= 1448.96+4.591\theta-0.05304\theta^2+0.0002374\theta^3 \\ &+ 1.340(S-35)+0.0163z+1.675\times10^{-7}z^2 \\ &- 0.01025\theta(S-35)-7.139\times10^{-13}\theta z^3. \end{aligned} \tag{4}$$

This equation is valid for $0\leq\theta\leq30^o$C, $30\leq S\leq40$ parts per thousand and $0\leq z\leq8000$ m.

The available bandwidth and transmission range for UWA communication depend on the signal-to-noise ratio (SNR) which is determined by the attenuation and noise level. The fact that the attenuation increases with frequency while the ambient noise decays with frequency makes the SNR vary over the signal bandwidth [7]. The SNR of an underwater acoustic signal can be expressed as follows [7]

$$SNR(x,f) = \frac{S_{tx}(f)}{N_{psd}(f)A(x,f)}, \tag{5}$$

where $S_{tx}(f)$ is the PSD of the transmitted signal.

The acoustic link can be classified as vertical or horizontal depending on the direction of the acoustic wave with respect to the sea floor. While carefully positioned vertical channels tend to suffer less from time dispersion, horizontal channels may exhibit long multipath delay spreads which can span over tens or even hundreds of milliseconds depending on the depth and distance between the transmitter and receiver [12]. The frequency response of the rth path in a multipath channel is expressed as [13]

$$H_r(f) = \frac{\Gamma_r}{\sqrt{A(x_r,f)}}, \tag{6}$$

where x_r is the length of the rth path which can be calculated using plane geometry and Γ_r is the cumulative reflection coefficient along the rth propagation path [7]. Given that each path has a delay τ_r, the overall frequency response is expressed as [7]

$$H(f) = \sum_r H_r(f)e^{-j2\pi f\tau_r}, \tag{7}$$

and the impulse response is given by

$$h(t) = \sum_r h_r(t-\tau_r), \tag{8}$$

where $h_r(t)$ is the inverse Fourier transform of $H_r(f)$.

A baseband model of the time-varying UAC with N_{path} discrete multipath components can be represented as follows [8]

$$h(\tau,t)= \sum_{r=1}^{N_{path}} \Psi_r(t)\delta(\tau-[\tau_r-\xi_r t]). \tag{9}$$

where $\Psi_r(t)$ represents the time-varying amplitude of the rth path and $\xi=v_{rel}/v$ is a Doppler scale factor that can be applied to each path. v_{rel} is the relative speed between the transmitter and receiver. If the underwater vehicle is moving a few m/s, this factor can be as high as 10^{-3} and hence the Doppler effect is regarded as non-negligible [7].

III. System Model

A. Single-Input Single-Output (SISO)-FBMC/OQAM

In FBMC/OQAM, real PAM symbols are transmitted on each subcarrier and since the duration of the real symbols is half that of OFDM/QAM, we obtain the same spectral efficiency as with OFDM (without the CP). The orthogonality condition in FBMC/OQAM is relaxed to the real field and this allows pulse shaping filters which have good time and

frequency localization to be used. The discrete-time transmitted FBCM/OQAM signal at the synthesis filter bank (SFB) output is given by [14]

$$s(l)=\sum_{m=0}^{M-1}\sum_{n} d_{m,n}\underbrace{g(l-n\frac{M}{2})e^{j\frac{2\pi}{M}m(l-\frac{L_g-1}{2})}e^{j\phi_{m,n}}}_{g_{m,n}(l)}, \quad (10)$$

where M is the number of subcarriers, $d_{m,n}$ represent the OQAM symbols for the mth subcarrier and nth symbol time, $\phi_{m,n}=\phi_0+\frac{\pi}{2}(m+n) \mod \pi$ (ϕ_0 can have an arbitrary value) and g is the impulse response of the prototype filter which has a length of $L_g=KM$ for an overlapping factor of K. It is to be noted that $g_{m,n}$ is orthogonal only in the real field. Thus, imaginary interference is inherent in an FBMC/OQAM system and is expressed as [14]

$$\sum_{l} g_{m,n}(l)g^{\star}_{p,q}(l)=\jmath\langle g\rangle^{p,q}_{m,n}, \quad (11)$$

where $\langle g\rangle^{p,q}_{m,n}=-\jmath\langle g_{m,n}|g_{p,q}\rangle$ and $\langle g_{m,n}|g_{p,q}\rangle$ is purely imaginary for $(m,n)\neq(p,q)$ [15]. If the number of subcarriers is large enough such that each subcarrier experiences flat fading and assuming that the channel is constant over the duration of the prototype filter, then the output of the analysis filter bank (AFB) at the pth subcarrier and qth FBMC/OQAM symbol can be represented as [14]

$$y_{p,q}=H_{p,q}d_{p,q}+\underbrace{\jmath\underbrace{\sum_{m=0}^{M-1}\sum_{n}}_{(m,n)\neq(p,q)} H_{m,n}d_{m,n}\langle g\rangle^{p,q}_{m,n}}_{I_{p,q}}+\eta_{p,q}, \quad (12)$$

where $H_{p,q}$ is the channel frequency response (CFR), $I_{p,q}$ and $\eta_{p,q}$ are the interference and noise terms respectively. If a prototype filter which is well localized in time and frequency is used, it can be assumed that the interference is due to only the first-order neighbors of the frequency-time points (FT) (p,q), i.e. $\Omega_{p,q}=\{(p\pm1,q\pm1),(p,q\pm1),(p\pm1,q)\}$ [14]. Moreover, if the CFR is also constant over the first-order neighbors, the expression in (12) is approximated as follows [14]

$$y_{p,q}\approx H_{p,q}c_{p,q}+\eta_{p,q}, \quad (13)$$

where

$$c_{p,q}=d_{p,q}+\underbrace{\jmath\sum_{(m,n)\in\Omega_{p,q}} d_{m,n}\langle g\rangle^{p,q}_{m,n}}_{u_{p,q}}=d_{p,q}+\jmath u_{p,q}, \quad (14)$$

and

$$u_{p,q}=\sum_{(m,n)\in\Omega_{p,q}} d_{m,n}\langle g\rangle^{p,q}_{m,n}. \quad (15)$$

$u_{p,q}$ represents the imaginary interference from the neighboring FT points. By transmitting known pilots at a given FT point and its neighborhood $\Omega_{p,q}$, the CFR estimate is obtained as follows [14]

$$\hat{H}_{p,q}=\frac{y_{p,q}}{c_{p,q}}\approx H_{p,q}+\frac{\eta_{p,q}}{c_{p,q}}. \quad (16)$$

0	1	0	1	0		0	1	0	-1	0
0	-j	0	-j	0		0	-j	0	j	0
0	-1	0	-1	0		0	-1	0	1	0
0	j	0	j	0		0	j	0	-j	0
0	1	0	1	0		0	1	0	-1	0
0	-j	0	-j	0		0	-j	0	j	0
0	-1	0	-1	0		0	-1	0	1	0
0	j	0	j	0		0	j	0	-j	0
	(a)						(b)			

Fig. 1. 2 x N_r IAM-C preamble (M=8) (a) Transmit Hydrophone 1 (b) Transmit Hydrophone 2

B. MIMO-FBMC/OQAM

The above concept can be easily applied to a MIMO system with N_t transmit and N_r receive hydrophones. Thus the signal at each receive hydrophone can be written as [14]

$$y^j_{p,q}=\sum_{i=1}^{N_t} H^{j,i}_{p,q}c^i_{p,q}+\eta^j_{p,q}, \quad j=1,2,\cdots,N_r \quad (17)$$

where $H^{j,i}_{p,q}$ is the M-point CFR from the ith transmit hydrophone to the jth receive hydrophone, $c^i_{p,q}$ and $\eta^j_{p,q}$ are the transmitted virtual symbol and noise respectively. The overall expression for a MIMO-FBMC/OQAM system is given by [14]

$$\boldsymbol{y}_{p,q}=\boldsymbol{H}_{p,q}\boldsymbol{c}_{p,q}+\boldsymbol{\eta}_{p,q}, \quad (18)$$

where

$$\boldsymbol{y}_{p,q}=\begin{bmatrix}y^1_{p,q} & y^2_{p,q} & \cdots & y^{N_r}_{p,q}\end{bmatrix},$$

$$\boldsymbol{\eta}_{p,q}=\begin{bmatrix}\eta^1_{p,q} & \eta^2_{p,q} & \cdots & \eta^{N_r}_{p,q}\end{bmatrix}^T,$$

$$\boldsymbol{H}_{p,q}=\begin{bmatrix}H^{1,1}_{p,q} & H^{1,2}_{p,q} & \cdots & H^{1,N_t}_{p,q}\\ H^{2,1}_{p,q} & H^{2,2}_{p,q} & \cdots & H^{2,N_t}_{p,q}\\ \vdots & \vdots & \ddots & \vdots\\ H^{N_r,1}_{p,q} & H^{N_r,2}_{p,q} & \cdots & H^{N_r,N_t}_{p,q}\end{bmatrix}.$$

The IAM-C (complex pilots) preamble proposed in [16] is used in this work. In order to estimate the CFR, we require at least $2N_t$+1 FBMC/OQAM symbol durations, while for MIMO-OFDM we would require N_t+$\frac{1}{2}$ complex symbol durations [14]. An example of the IAM-C preamble structure for a $2\times N_r$ MIMO system is shown in Fig. 1. The alternate zero vectors prevent the pilot vectors from being affected by interference from the data parts. By taking into account only the pilot vectors at timing instants q=1,3, the expression in (18) can be re-written as follows [14]

$$\begin{bmatrix}\boldsymbol{y}_{p,1} & \boldsymbol{y}_{p,3}\end{bmatrix}=\boldsymbol{H}_{p,1}\begin{bmatrix}c^1_{p,1} & c^1_{p,3}\\ c^2_{p,1} & c^2_{p,3}\end{bmatrix}+\begin{bmatrix}\boldsymbol{\eta}_{p,1} & \boldsymbol{\eta}_{p,3}\end{bmatrix}. \quad (19)$$

From the preamble structure in Fig. 1, one can notice that $c^1_{p,1}=c^1_{p,3}=c^2_{p,1}=-c^2_{p,3}\equiv c_p$ and hence

$$\begin{bmatrix}\boldsymbol{y}_{p,1} & \boldsymbol{y}_{p,3}\end{bmatrix}=\boldsymbol{H}_{p,1}c_p\boldsymbol{Q}_2+\begin{bmatrix}\boldsymbol{\eta}_{p,1} & \boldsymbol{\eta}_{p,3}\end{bmatrix}, \quad (20)$$

where $\boldsymbol{Q}_2$ is a Hadamard matrix of order N_t (two in this case). An estimate of the CFR matrix at the pth subcarrier is thus given by [14]

$$\hat{\boldsymbol{H}}_{p,1}=\begin{bmatrix}\boldsymbol{y}_{p,1} & \boldsymbol{y}_{p,3}\end{bmatrix}\frac{1}{c_p}\boldsymbol{Q}_2^{-1}. \quad (21)$$

TABLE I
CHANNEL PARAMETERS

Water depth	1000 m
Transmitter (TX) depth	999 m
Receiver (RX) depth	1 m
TX-RX Horizontal separation	5 m
Bandwidth	25 kHz
Carrier frequency	32.5 kHz

IV. PERFORMANCE EVALUATION

A. BER performance and bit rate

The vertical channel configuration parameters are given in Table I. It is assumed that the relative speed between the transmitter and receiver is 0.5 m/s. This may be caused by unintentional movement due to tides or sea currents. The maximum Doppler frequency in the UAC is approximately 11 Hz. The time-varying channel coefficients are obtained using a statistical model based on the maximum entropy principle [17] which only relies on a few parameters such as channel average power and Doppler spread to model. The channel impulse response (CIR) with a maximum delay spread of 2.6 ms and channel scattering function (CSF) as a function of delay (τ) and Doppler (ν) are shown in Fig. 2. The Doppler spread for the channel tap delays in Fig. 2 increases linearly from 0.5 Hz to 2 Hz. For the purpose of simulation, we used colored noise instead of additive white Gaussian noise (AWGN) since it better represents noise in an UAC. The simulation parameters for the MIMO OFDM and FBMC/OQAM systems are summarized in Table II. Considering the same transmission time, the BER performances for the MIMO-OFDM and MIMO-FBMC/OQAM systems in the vertical UAC are shown in Fig. 3. Each frame of a $2\times N_r$ FBMC/OQAM system consists of 5 real preamble symbols. As for the $4\times N_r$ FBMC/OQAM system, each frame consists of 9 real preamble symbols. For the $2\times N_r$ and $4\times N_r$ OFDM systems, the preamble lengths are 2 and 4 complex symbol durations, respectively. A simple one-tap equalizer is used for the MIMO-OFDM system while the MIMO-FBMC/OQAM receiver processing consists of a 3-tap equalizer [18]. A Hermite prototype filter with an overlapping factor of 4 is used for the FBMC systems.

It is observed that both the coded and uncoded MIMO-FBMC/OQAM systems outperform the MIMO-OFDM systems. This shows the robustness of FBMC against both time and frequency dispersions. With 1/2 rate Turbo code, the BER performances of both systems are greatly improved. For instance, at a BER of 10^{-4}, the Turbo-coded 2×12 and 4×12 FBMC/OQAM systems outperform the Turbo-coded OFDM systems by 4 dB in both cases.

For the bit rate computation, the parameters as given in Table II are assumed. The theoretical bit rates that can be achieved with the different systems in the 1000 m vertically configured UAC are given in Table III. For similar parameters, the $2\times N_r$ and $4\times N_r$ FBMC/OQAM systems achieve about 17% and 25% higher bit rate than the $2\times N_r$ and $4\times N_r$ OFDM systems respectively.

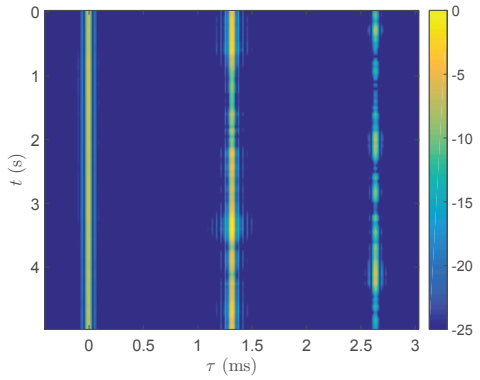

(a)

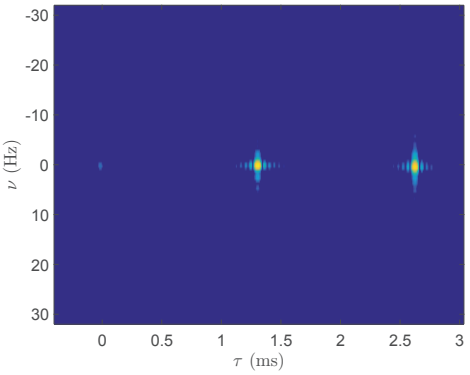

(b)

Fig. 2. Underwater Acoustic Channel (a) CIR (b) CSF

TABLE II
BIT RATE COMPUTATION PARAMETERS

Bandwidth (kHz)	25
Subcarriers	512
Complex Symbol duration (ms)	20.48
OFDM CP duration (ms)	5.12
Modulation	16-QAM
FEC code rate	0.5

B. Video Transmission in an UAC

While MPEG-4 has been used for underwater wireless video transmission in UACs (e.g [19]–[21]) and has achieved real-time low resolution video transmission with satisfactory quality, more efficient video compression standards are available now. These include H.264 (MPEG-4 Part 10 AVC) and High Efficiency Video Coding (HEVC). In this work we consider the H.264/AVC standard for video compression ahead of High Efficiency Video Coding (HEVC). For the same bit rate, HEVC is known to achieve a better video quality than H.264/AVC. However, for a target bit rate HEVC uses a complex prediction process to remove the redundant information in the video and minimize the coding distortion [22]. Hence, it has a higher computational complexity than H.264/AVC and is more efficient when the video is encoded in non real-time.

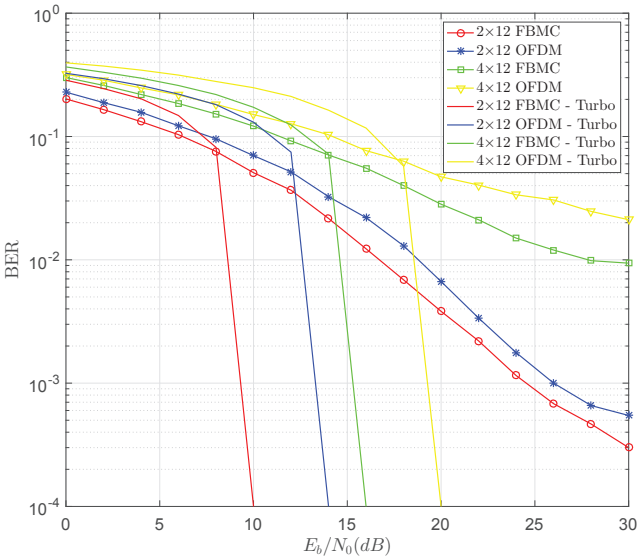

Fig. 3. BER performance of MIMO OFDM & FBMC/OQAM systems

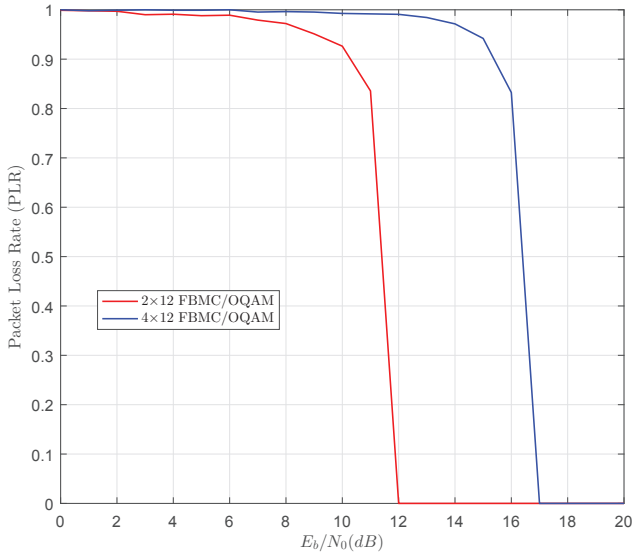

Fig. 4. Packet Loss Rate for the 2×12 & 4×12 FBMC/OQAM systems

TABLE III
THEORETICAL BIT RATE ($kbps$)

MIMO configuration	OFDM	FBMC/OQAM
$2\times N_r$	63.1	73.7
$4\times N_r$	84.2	105.2

For the video transmission part we consider the Turbo-coded MIMO-FBMC/OQAM systems in Table III since they not only achieve higher bit rates than the MIMO-OFDM systems but also a better error performance. We consider an uncompressed standard definition (SD) video with a resolution of 640×480, frame rate of 30 fps and duration 12 s. The video stream (365 frames) is compressed to target bit rates of 70 kbps and 100 kbps for the $2\times N_r$ and $4\times N_r$ FBMC/OQAM systems respectively. Frequent coding of the I-frames avoids propagation of errors between frames, thereby improving the error resilience of the video streams. Hence, a short intra-period of 8 is used. The maximum packet size is set at 800 bytes and the number of reference frames for video coding is set at 5, which is adequate for practical implementations [23].

1) Frame Rate Computation: The average number of bits per frame for the video streams compressed at 70 kbps and 100 kbps are 2,355 and 3,364 respectively. It is to be noted that the I-frames consist of more bits than the P and/or B video frames. Assuming the maximum supported capacity of the systems, the calculated frame rate for the $2\times N_r$ and $4\times N_r$ FBMC/OQAM systems is 31.3 fps in both cases. This value is greater than the original frame rate of 30 fps, implying real-time transmission is theoretically feasible.

2) Packet Loss: The H.264/AVC bitstreams are encoded in 502 and 543 video packets for the $2\times N_r$ and $4\times N_r$ FBMC/OQAM systems respectively. Fig. 4 shows the Packet Loss Rate (PLR) for the two systems. The PLR is zero at E_b/N_0 values of 12 dB and 17 dB for $2\times N_r$ and $4\times N_r$ systems respectively.

3) Peak-Signal-to-Noise-Ratio (PSNR): The graph in Fig. 5 shows the received video quality for the systems under investigation. We assess the received video quality using the Peak Signal-to-Noise Ratio (PSNR) metric. The latter is a simple method to evaluate the quality of video streams, although it may not always reflect the human viewer's judgment of the quality. This method generally compares an original uncompressed video with one which has been compressed (or processed in other ways). We use frame copy error concealment technique in order to cope with partial or complete loss of frames due to packet loss. For low bit rate video compression, it is very likely that a whole video frame is encoded within a single packet. In this case, a number of bit errors distributed across the video stream may cause too many packet loss (and therefore frame loss), making error concealment techniques ineffective. The range of E_b/N_0 values shown in Fig. 5 denotes a maximum PLR of 25% for each system. Beyond this value, the video quality is so severely degraded that no useful information can be extracted from the received videos. The higher the supported bit rate of the system, the better is the video quality (higher PSNR), as can be observed for the $4\times N_r$ system when packet loss is negligible.

V. CONCLUSION

In this work we have seen that FBMC/OQAM provides a better error performance than OFDM in a time-varying UAC since it is based on a pulse-shaping filter with good time and frequency localization features. Furthermore, FBMC/OQAM achieves a higher bit rate than OFDM for the same bandwidth since it does not include a CP. High data rates are desirable

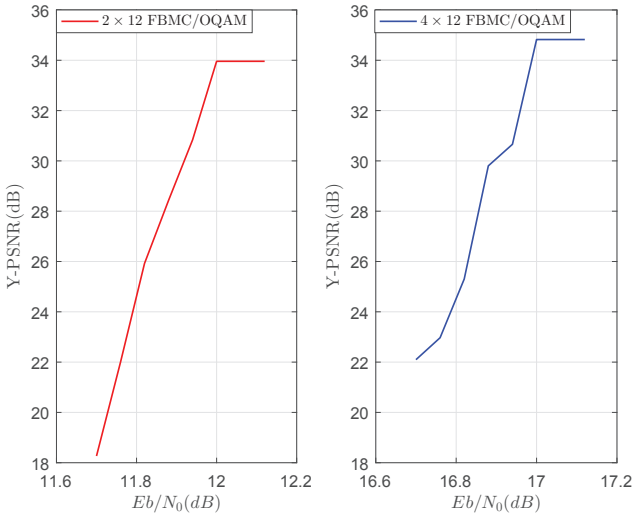

Fig. 5. Received video quality in terms of PSNR (dB) for the 2×12 & 4×12 FBMC/OQAM systems

for modern underwater applications involving wireless video transmission. The bit rates obtained with the FBMC/OQAM systems over the 1000 m vertical acoustic link are sufficiently high to transmit a video with acceptable quality in real-time.

REFERENCES

[1] B. Li *et al.*, "MIMO-OFDM for high-rate underwater acoustic communications," *IEEE Journal of Oceanic Engineering*, vol. 34, no. 4, pp. 634–644, Oct. 2009.

[2] A. Aminjavaheri and B. Farhang-Boroujeny, "UWA massive MIMO communications," in *OCEANS 2015 - MTS/IEEE Washington*, Oct 2015, pp. 1–6.

[3] J. Gomes and M. Stojanovic, "Performance analysis of filtered multitone modulation systems for underwater communication," in *OCEANS 2009, MTS/IEEE Biloxi-Marine Technology for Our Future: Global and Local Challenges*. IEEE, 2009, pp. 1–9.

[4] P. Amini, R.-R. Chen, and B. Farhang-Boroujeny, "Filterbank multicarrier communications for underwater acoustic channels," *Oceanic Engineering, IEEE Journal of*, vol. 40, no. 1, pp. 115–130, 2015.

[5] A. Aminjavaheri, A. RezazadehReyhani, and B. Farhang-Boroujeny, "Frequency spreading Doppler scaling compensation in underwater acoustic multicarrier communications," in *Communications (ICC), 2015 IEEE International Conference on*, Jun. 2015, pp. 2774–2779.

[6] E. V. Zorita and M. Stojanovic, "Space –frequency block coding for underwater acoustic communications," *IEEE Journal of Oceanic Engineering*, vol. 40, no. 2, pp. 303–314, Apr. 2015.

[7] M. Stojanovic and J. Preisig, "Underwater acoustic communication channels: Propagation models and statistical characterization," *IEEE Communications Magazine*, vol. 47, no. 1, pp. 84–89, Jan. 2009.

[8] H. Esmaiel and D. Jiang, "Review article: Multicarrier communication for underwater acoustic channel," *Int'l J. of Communications, Network and System Sciences*, vol. 6, no. 08, p. 361, 2013.

[9] W. H. Thorp, "Analytic description of the low-frequency attenuation coefficient," *The Journal of the Acoustical Society of America*, vol. 42, no. 1, pp. 270–270, 1967.

[10] F. Fisher and V. Simmons, "Sound absorption in sea water," *The Journal of the Acoustical Society of America*, vol. 62, no. 3, pp. 558–564, 1977.

[11] M. C. Domingo, "Overview of channel models for underwater wireless communication networks," *Physical Communication*, vol. 1, no. 3, pp. 163–182, 2008.

[12] T. Melodia, H. Kulhandjian, L.-C. Kuo, and E. Demirors, "Advances in underwater acoustic networking," *Mobile ad hoc networking: Cutting edge directions*, vol. 852, 2013.

[13] M. Stojanovic, "Underwater acoustic communications: Design considerations on the physical layer," in *Wireless on Demand Network Systems and Services, 2008. WONS 2008. Fifth Annual Conference on*. IEEE, 2008, pp. 1–10.

[14] E. Kofidis and D. Katselis, "Preamble-based channel estimation in MIMO-OFDM/OQAM systems," in *Proc. IEEE Int Signal and Image Processing Applications (ICSIPA) Conf*, Nov. 2011, pp. 579–584.

[15] C. Lélé *et al.*, "Channel estimation methods for preamble-based OFDM/OQAM modulations," *European Transactions on Telecommunications*, vol. 19, pp. 741–750, 2008.

[16] J. Du and S. Signell, "Novel preamble-based channel estimation for OFDM/OQAM systems," in *Proc. IEEE Int. Conf. Communications*, Jun. 2009, pp. 1–6.

[17] F. X. Socheleau, C. Laot, and J. M. Passerieux, "A maximum entropy framework for statistical modeling of underwater acoustic communication channels," in *Proc. OCEANS 2010 IEEE - Sydney*, May 2010, pp. 1–7.

[18] T. Ihalainen, A. Ikhlef, J. Louveaux, and M. Renfors, "Channel equalization for multi-antenna FBMC/OQAM receivers," *IEEE Transactions on Vehicular Technology*, vol. 60, no. 5, pp. 2070–2085, Jun 2011.

[19] J. Ribas, D. Sura, and M. Stojanovic, "Underwater wireless video transmission for supervisory control and inspection using acoustic OFDM," in *OCEANS 2010*, Sep. 2010, pp. 1–9.

[20] L. D. Vall, D. Sura, and M. Stojanovic, "Towards underwater video transmission," in *Proceedings of the Sixth ACM International Workshop on Underwater Networks*. ACM, 2011, p. 4.

[21] R. Ahmed, L. D. Vall, M. Stojanovic, and R. Narayanaswami, "Video transmission over an in-air acoustic link," *In Proc. Workshop on Underwater Networks (WUWNet)*, Dec. 2011.

[22] A. Aldahdooh, M. Barkowsky, and P. L. Callet, "Spatio-temporal error concealment technique for high order multiple description coding schemes including subjective assessment," in *2016 Eighth International Conference on Quality of Multimedia Experience (QoMEX)*, June 2016, pp. 1–6.

[23] H. Hadizadeh and I. V. Bajic, "NAL-SIM: An interactive simulator for H.264/AVC video coding and transmission," in *2010 7th IEEE Consumer Communications and Networking Conference*, Jan 2010, pp. 1–2.